Proceedings of the ASME 2010 3rd Joint US-European Fluids Engineering Summer Meeting and 8th International Conference on Nanochannels, Microchannels, and Minichannels
FEDSM-ICNMM2010
August 1-5, 2010, Montreal, Canada

FEDSM-ICNMM2010-30485

UNSTEADY FLOW NUMERICAL ANALYSIS OF NEW-TYPE DEEP WELL PUMP UNDER MULTI-CONDITIONS

LU Wei-gang luweigang@ujs.edu.cn
ZHOU Ling zhouling6617@163.com
ZHANG De-sheng desheng1982@163.com
ZOU Ping-ping zpp.87.08@163.com
Wang Chuan wangchuan198710@126.com

Technical and Research Center of Fluid Machinery Engineering,Jiangsu University,Jiangsu,China

ABSTRACT

The interaction between impeller and guide vane of the deep well pump is one of the most important factors which cause the pressure fluctuation in the channels. However, even nowadays some flow events in the deep well pump are still under study and far from fully understood. So the unsteady flow field of a two-stage deep well pump was simulated with FLUENT code based on sliding mesh and the RNG k-ε turbulence model, to investigate the pressure fluctuation by interactions between the impeller and guide vane. The computing domain extends from the inlet of the first stage deep well pump to the outlet of the second stage guide vane. With the Fast Fourier Transform (FFT) analysis, the pressure fluctuation and frequency fluctuation are analyzed under multi-conditions. In this paper, the pressure fluctuation differences between the first stage and secondary are also compared. The numerical results show that the pressure fluctuates at the blade passage frequency, and the maximum amplitude of blade passage frequency occurs in the region from the rotor to the stator when the impeller blade gets close to the guide vane trailing edge, but it decreases rapidly after fluid entering the guide vane. Compared with the steady simulation, the averaged calculated single-stage head of unsteady simulation is more accord with the reality, which is less than the tested head with a relative deviation of 5%.

INTRODUCTION

Submersible pump for deep well, widely used in the countryside, mines, geothermal utilization and so on, are the main equipment for pumping underground water [1].

Due to the working conditions, the pump diameter is limited by the well diameter, and the single-stage head designed by traditional methods is low. In order to increase the single-stage head, t the maximum impeller diameter design method was created by Lu Weigang [2]. A series of submersible pumps designed by this method were manufactured and tested. These pumps are of a new frame, compared with the similar products at domestic and international markets, the single-stage head increases by 20% to 50%, the efficiency increases by 3% to 9%, and the whole axial length and weight decreases around 1/3. The productions show good energy saving and material saving characters and can replace traditional pumps for deep well in the future. Shi Weidong et al. [3] simulated of the internal steady flow of this type well pump, and analyzed its hydraulic design. Zhang Qihua et al. [4] and Shi Weidong et al. [5] studied the axial force in the deep well pump, and confirmed that maximum diameter design method can effectively balance the impeller axial force without reducing the head and efficiency.

At present, the unsteady flow have many in-depth studies for the volute impeller centrifugal pump [6, 7], axial flow pump [8], double suction pumps [9] and so on, but there was not any relevant unsteady flow research of deep well pumps. This Rotor- Stator Interaction (RSI) is the consequence of the

interaction between the rotating flow perturbations caused by the impeller blades and the flow perturbation caused by the guide vanes. This interaction induces pressure waves that propagating in the entire flow regions. This interaction is one of the main causes of vibration, noise, fissures, blade or guide vanes cracking bearing ruins in well pumps.

NOMENCLATURE

Q_N Flow rate (m^3/h)
H Head (m)
η Efficiency (%)
n Rotation speed (r/min)
P_s Static pressure (Pa)
θ The impeller passage angle (°)
n_s Specific speed= $\frac{3.65n\sqrt{Q}}{H^{3/4}} = \frac{3.65.r/\min\sqrt{m^3/s}}{m^{3/4}}$

THE GEOMETRIC MODEL OF THE DEEP WELL PUMP

The pump for deep well tested is the 150QJ20 model, which is used in the State Hi-tech Research and Development Program of China (No.2006AA100211). The characteristics at the design condition are: Q_N =20m^3/h, single-stage H=11m, n=2850r/min. ns=128. The impeller was designed by the maximum impeller diameter design method created by Lu Weigang in 2004.

The main innovations of the maximum impeller diameter design method are as follows:

(1)The diameter of impeller front shroud is almost the same as the pump's casing inner diameter. The diameter of impeller back shroud is the middle of guide vane shroud and impeller front shroud, which improved the single-stage impeller head and pump efficiency.

(2) The shape of impeller front shroud is like a cone around the pump shaft. The flow out from impeller has an medial trend can result in a higher efficiency, while not increasing the length of pump .In order to shorten the length of the pump further, the back shroud is designed perpendicular to the pump shaft.

(3)The face seal is used at the inlet of the impeller, impeller and pump shaft is of clearance fit. Since the area of front shroud is almost the same as back shroud's, axial force on the impeller is self-balanced.

(4) The blades inlet is extended as much as possible, and streamline along the back shroud is designed to be longer than front shroud to avoid the secondary reflux at impeller outlet.

(5) Blades outlet angle is determined by making pump have the characteristics of non-overload.

The impeller has 7 blades; its axial projection drawing and solid model created using Pro/E are shown in Fig. 1.

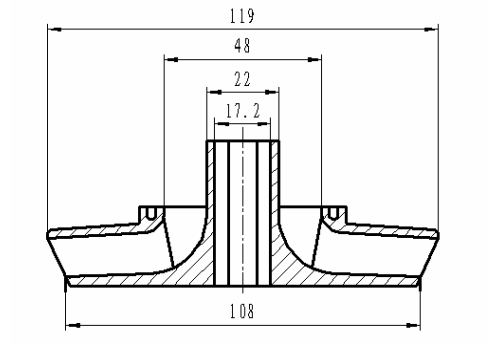

(a) Axial projection drawing

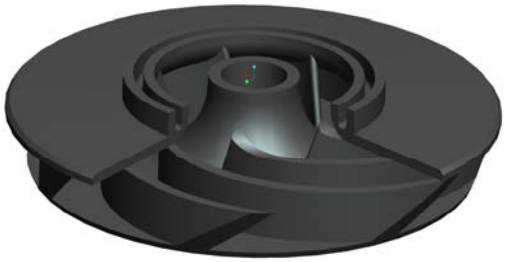

(b) Solid model

Fig. 1 Impeller

A new return guide vane with twisted inlet and 3D curved surface was designed to reduce the cost, and the hydraulic loss, its axial projection drawing and the solid model are shown in Fig. 2.

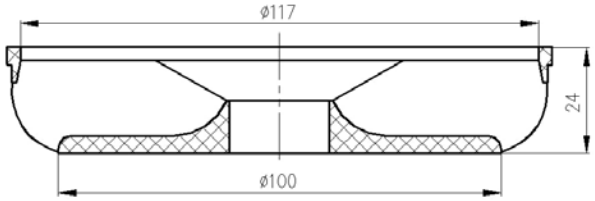

(a) Axial projection drawing

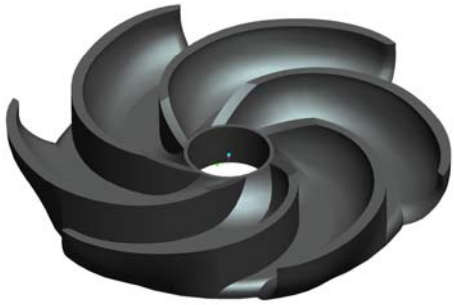

(b) Solid model

Fig. 2 Twisted return guide vane

ROTOR-STATOR NUMERICAL SIMULATION

The computing domain corresponds to the two stages deep well pump extending from the inlet of the first stage to the outlet of the second stage guide vane. These parts are shown in the assembly drawing, Fig. 3.

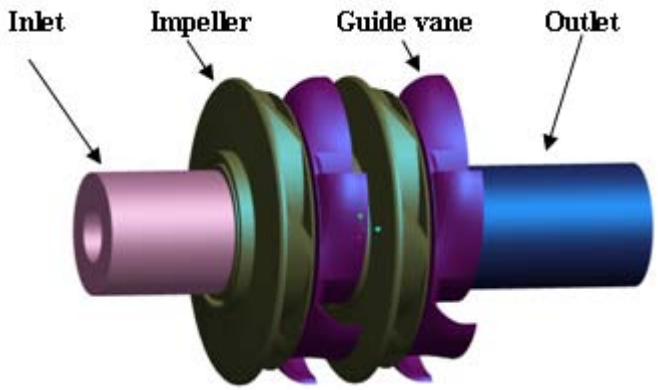

Fig. 3 Assembly drawing

The whole flow channel consists of four parts: inlet water segment, impeller, guide vane, outlet water segment.

The whole mesh generation process is carried out with the GAMBIT 2.2 software. Table 1 show the analysis of grid sensitively, when the grids size less than 1.4 or grids number greater than 1.29 million, the numerical simulation results showing a stable state, that the single-stage head and the efficiency change little. So integrated computer's configuration, use the grids size of 1.4 to carry out the related follow study. The mesh characteristics for each component are summarized in Table 2. A general view of the meshes is given in Fig. 4.

Table 1 Grid sensitively analysis

Grids Size	1.2	1.4	1.6	1.8	2
Grids Number	1988698	1292031	897182	692131	504931
Efficiency η/%	67.3269	67.3264	67.3123	66.2572	66.2727
Single-stage Head H/m	11.996	11.989	11.941	11.939	11.721

Table 2 Mesh characteristics of the computing domain

Components	Grids Size	Grids Number	Mesh Software
Inlet	1.4	153308	
Impeller	1.4	195026	
Guide vane	1.4	235165	GAMBIT 2.2
Outlet	1.4	278941	
Total		1292031	

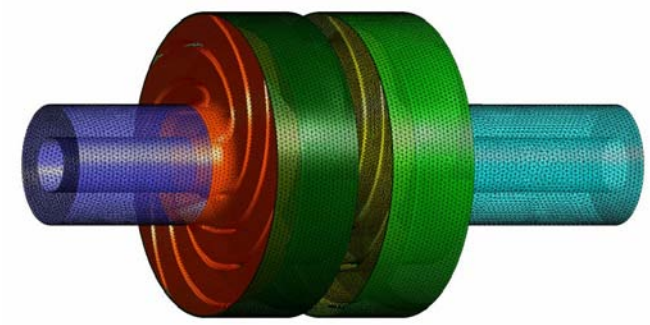

Fig. 4 Calculation mesh

The unsteady simulation was performed with Standard k-ε turbulence model implemented in the FLUENT 6.2 code. The standard wall functions were used to simulate the boundary layers. The second order implicit scheme is adopted for the turbulent simulation. Control equations are discredited in both space and time domain. SIMPLEC arithmetic is used to solve the pressure and velocity coupling at each time step. The time step corresponds to 1°of the impeller rotation, 360 time steps should be calculated in one cycle of rotor. Numerical convergence is set to 10^{-5} and periodicity solution is fulfilled after five impeller revolutions. The types of boundary conditions are summarized in Table 3.

Table 3 Boundary conditions

B.C	Location	Option
Inlet	First stage impeller inlet	Velocity Inlet
Outlet	Secondary guide vane outlet	Outflow
Wall	Solid surfaces	Standard Wall Functions

NUMERICAL RESULTS AND ANALYSIS

One of the key parameters for potential interaction is the clearance gap between guide vanes and impeller blades, It affects the intensity of rotor-stator interactions. The strong-coupling evolution of static pressure in the secondary stage at different conditions is shown in Fig.5. The potential interaction is amplified when the impeller blade faces to the guide vane trailing edge, and the static pressure evolution at off-design conditions is stronger than that at design conditions. In this paper θ is defined as the impeller passage angle. The evolution of static pressure is about the cycle of 52 °, with the same impeller rotation cycle. In the $0.8Q_N$, the impeller exit appeared serious water impact, and a clear area of low pressure emerged at the entrance of the guide vane. With the flow rate increased，the area of low pressure decrease gradually. Vortex generated in the middle of the guide vane, shows the guide vanes' design unreasonable, and has room to be improved.

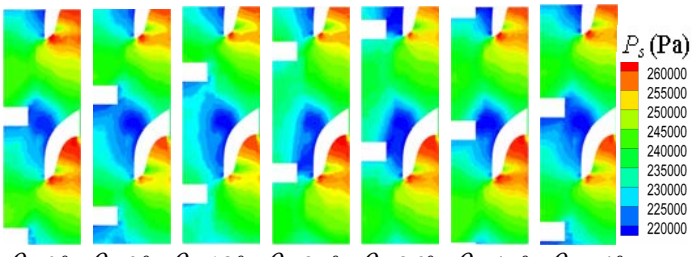

(a) $0.8Q_N$

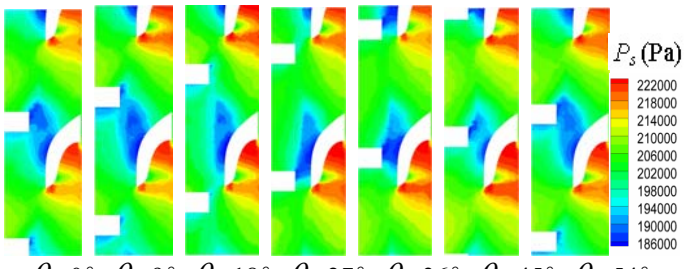

(b) $1.0Q_N$

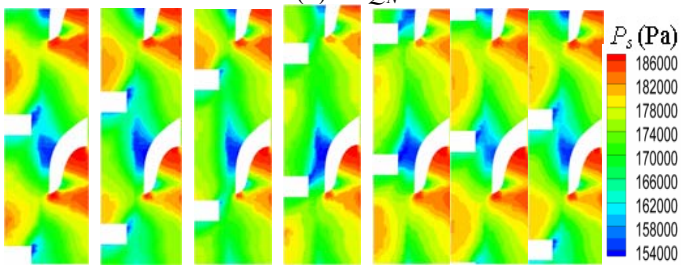

(c) $1.2Q_N$

Fig. 5 The static pressure evolution under multi-conditions

The locations of the pressure monitoring points in the flow channel is shown in Fig. 6. The pressure coefficient fluctuation is defined below:

$$c_p = \frac{p - \overline{p}}{\frac{1}{2}\rho U^2} \tag{1}$$

where p is the pressure, $\overline{p}$ the average pressure for one impeller revolution and U is the impeller peripheral velocity.

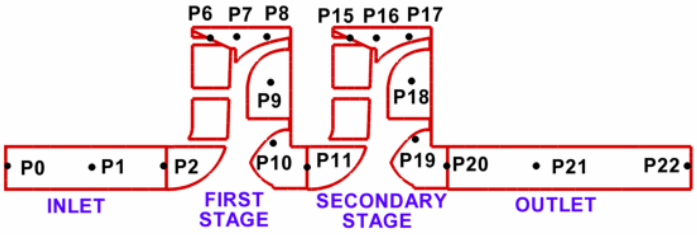

Fig. 6 Locations of the monitoring points in cross-section

The pressure fluctuation for half impeller revolution from inlet to tip at blade inlet is shown in Fig.7. The pressure fluctuation data of one impeller revolution is analyzed by Fast Fourier Transform (FFT) to obtain the amplitudes of the harmonic components. Fig.8 presents the frequency spectra of the pressure coefficient at the mentioned points.

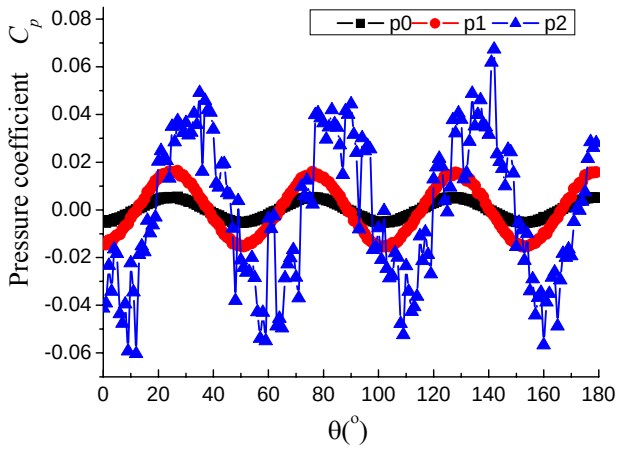

Fig. 7 Pressure fluctuation of monitoring points at rotor inlet

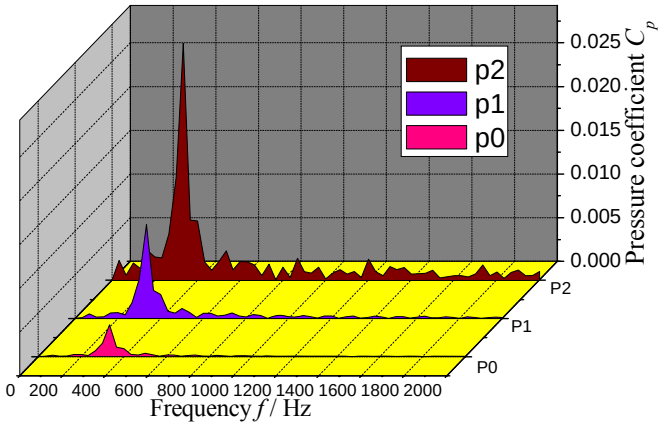

Fig. 8 Frequency spectra of pressure coefficient of monitoring points at rotor inlet

The fluctuating features of points (P0 to P2) at impeller inlet are almost coincident with each other, and they all have 7 picks and 7 valleys in one impeller revolution, which is same to the blade number of impeller. The most significant discrepancy of pressure amplitude arises at different position. The more close to the impeller, the more intense of the pressure fluctuation. From pump inlet to the impeller inlet, the pressure coefficient fluctuation amplitude increases gradually. The spectral analysis highlights the different stems from the pressure amplitude value at the impeller blade passing frequency (BPF). The frequency spectra of the pressure coefficient show the pressure amplitudes correspond to the blade passing frequency. It is found that the dominant frequency at the monitoring points of the rotor inlet all takes the same value of 333 Hz, which is approximately equal to the BPF (333.5 Hz).

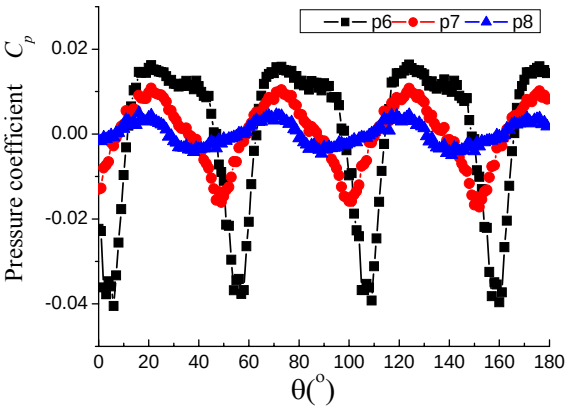

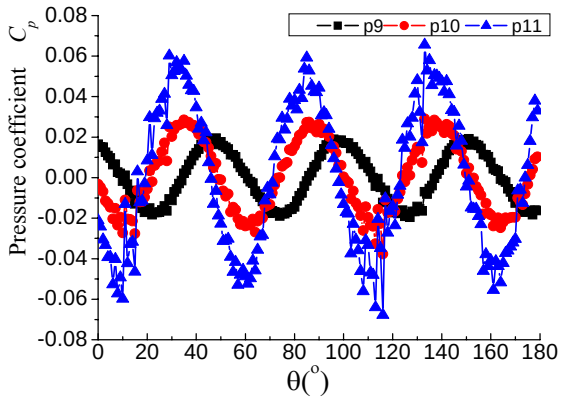

(a) Pionts in first stage

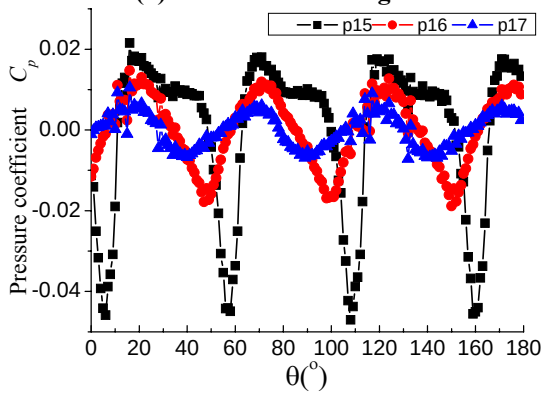

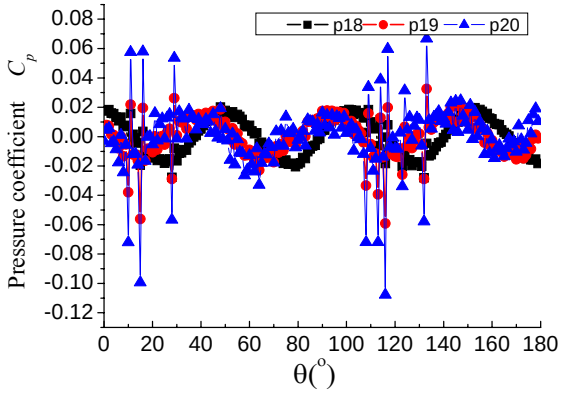

(b) Pionts in secondaty stage

Fig. 9 Pressure fluctuation of monitoring points

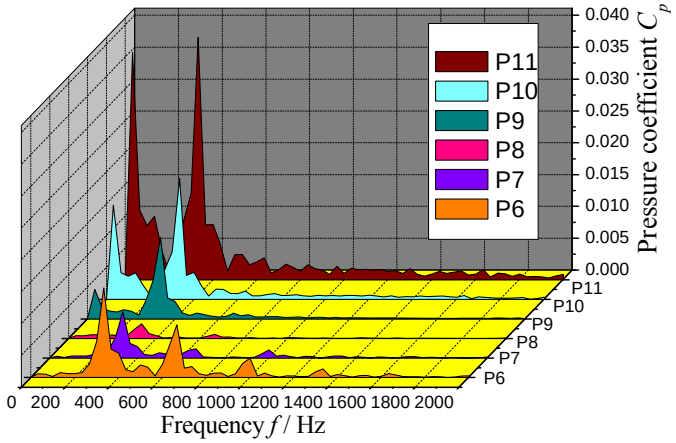

(a) Pionts in first stage

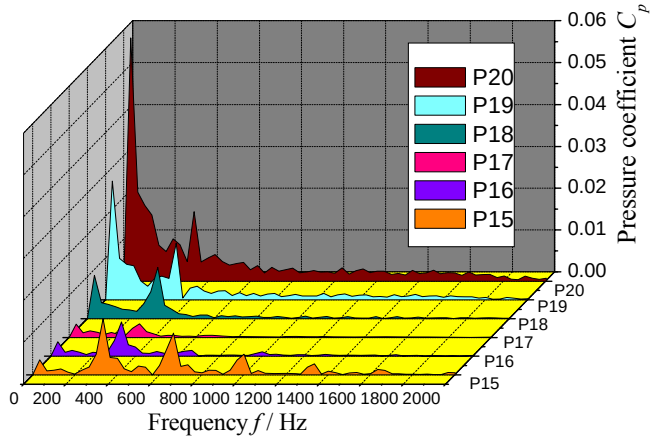

(b) Pionts in secondaty stage

Fig. 10 Frequency spectra of pressure coefficient of monitoring points

The pressure fluctuations for a half period from inlet to outlet are shown in Fig.9. Fig.10 presents the frequency spectra of the pressure coefficient at the mentioned points. The pressure fluctuation show differences between the stages. Similar pressure fluctuations appeared in the impeller outlet of the two stages (p6 p7 p8 and p15 p16 p17), but the pressure fluctuations in the guide vane (p9 p10 p11 and p18 p19 p20) show a quite different situation. It may be caused by different outflow conditions, and the outflow condition of the secondary stage (p18 p19 p20) is free flow. In the whole flow channel, the impeller outlet (p6 and p15) is the most volatile places of the pressure, and also is the places of generating the Rotor- Stator Interaction.

Figure 11 shows the single stage head obtained by steady and unsteady numerical simulation compared with test values. Compared with the steady simulation, the averaged calculated single-stage head obtained by unsteady simulation is more accord with the reality, which is less than the tested head. The error is within 5%.

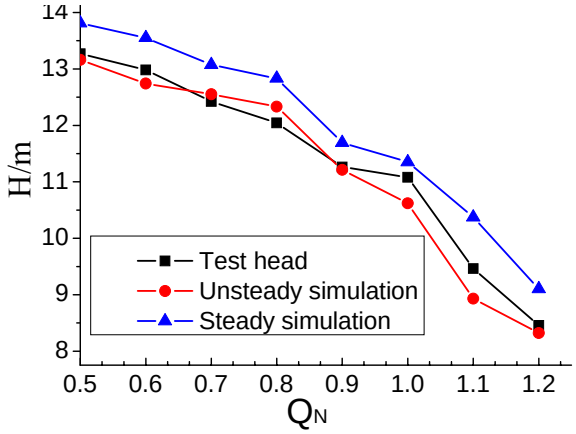

Fig. 11 The comparison of single-stage head

CONCLUSIONS

The interaction between impeller and guide vane in a deep well pump is one of the most important factors which cause the pressure fluctuation in the channels. The rotor stator interactions have been investigated in the case of a two stage deep well pump, featuring 7 rotor blades and 6 guide vanes. The most important potential interaction aggravates when the impeller blade is getting close to the guide vane trailing edge. In the whole flow channel, the impeller outlet is the most volatile regions of the pressure, and also is the locations of generating the Rotor- Stator Interaction. Compared with the steady simulation, the averaged calculated single-stage head of unsteady simulation is more accord with the reality. In this case, unsteady simulation could be used in the prediction of pumps' performance.

ACKNOWLEDGMENTS

The work was supported by the grant from the State Hi-tech Research and Development Program of China (No.2006AA100211).

REFERENCES

[1] Shi Weidong, Wang Hongliang, et al, 2009, "Development and prospect of deep well pump in China," Drainage and Irrigation Machinery., Vol. 27(1), pp.64-68.

[2] Shi Weidong, Lu Weigang, Wang Hongliang, Li Qifeng, 2009, "Research on the Theory and Design Methods of the New Type Submerible Pump for Deep Well," ASME Fluids Engineering Division Summer Meeting and Exhibition., Aug 2-5, 2009, Vail, Colorado, USA

[3] Shi Weidong, Zhang Qihua, Lu Weigang, 2006, "Hydraulic design of new-type deep well pump and its flow calculation," Journal of Jiangsu University: Natural Science Edition., Vol. 27(6), pp.528-531.

[4] Zhang Qihua, Lu Weigang, Shi Weidong, 2007, "Numerical calculation of axial force and balancing on new type deep well pump," Drainage and Irrigation Machinery., Vol. 25(6), pp.7-10.

[5] Shi Weidong, Li Qifeng, Lu Weigang, et al, 2009, "Estimation and experiment of axial thrust in centrifugal pump based on CFD," Transactions of the Chinese Society for Agricultural Machinery., Vol. 40(1), pp.60-63.

[6] Barrio, Raúl, 2010, "Numerical analysis of the unsteady flow in the near-tongue region in a volute-type centrifugal pump for different operating points," Computers and Fluids., Vol.39, pp.859-870.

[7] González José, Blanco Eduardo, Santolaria Carlos, etc al, 2002, "Unsteady flow structure on a centrifugal pump: Experimental and numerical approaches," American Society of Mechanical Engineers, Fluids Engineering Division (Publication) FED., Vol.257(2B), pp.761-768.

[8] Zhang Desheng, Shi Weidong, Chen Bin, etc al, 2010, "Unsteady flow analysis and experimental investigation of axial-flow pump," Journal of Hydrodynamics., Vol.22 (1), pp.35-43.

[9] Gonzalez J, Oro JMF, Diaz KMA, etc al, 2009, "Unsteady flow patterns for a double suction centrifugal pump," Journal of Fluids Engineering-Transactions of the ASME., Vol.131 (7), pp.1102-1111.